Tellus (1996), 48A, 254–271
Printed in Belgium – all rights reserved

TELLUS
ISSN 0280–6495

Blocking as a wave-wave interaction

By C. WIIN CHRISTENSEN, *Danish Defense Command, Postbox 202, 2950 Vedbaek, Denmark*, and A. WIIN-NIELSEN, *Niels Bohr Institute for Astronomy, Physics and Geophysics, University of Copenhagen, Haraldsgade 6, 2200 Copenhagen N, Denmark*

(Manuscript received 24 February 1995; in final form 23 August 1995)

ABSTRACT

The paper investigates the possibility that blocking may be one of the multiple steady states that are possible in a low-order nonlinear system based on wave-wave interaction rather than zonal-wave interaction. The model is based on an equivalent barotropic system forced by a Newtonian forcing and dissipated by boundary layer friction. Three waves are permitted to interact in a nonlinear way giving a system of six nonlinear equations since each wave has a sine and a cosine component. The multiple steady states are determined by a mixture of analytical and numerical methods. The kinetic energy of each of these states is calculated, and the structure of the stable steady states is shown. It may be concluded that wave-wave interaction, just as interaction between the zonal flow and the waves, is a possible mechanism for the formation of blocking patterns. However, both mechanisms, expressed as interaction in low order systems, have difficulties in providing at the same time a fair comparison between theory and observations with respect to horizontal scale and levels of kinetic energy.

1. Introduction

Blocking is one of the well known quasi-stationary patterns in atmospheric flows. It is described from a synoptic point of view by Elliott and Smith (1949) and Berggren et al. (1949) and later also by a climatological and statistical study by Rex (1950). More recent observational studies of blocking in the northern and southern hemispheres have been conducted by Lejenäs and Økland (1983), and Lejenäs (1984). An overview of the recent state of observational, numerical and theoretical research on blocking may be found in Benzi et al. (1986). Early studies of blocking and related phenomena have been carried out by Egger (1978) who considered flow with and without interactions between the zonal flow and the eddies. The study by Vickroy and Dutton (1979) emphasized bifurcations and catastrophies in quasi-geostrophic flow under the influence of forcing and dissipation.

The first studies of multiple steady states in low-order, nonlinear systems by Charney and DeVore (1979) and Wiin-Nielsen (1979) emphasized the nonlinear interaction between the zonal flow and the eddies. A closer scrutiny of these solutions revealed that although a stable, steady state resembling a block could be found such a solution will in general have a level of kinetic energy that is quite high compared to the energy level found in real blocking situations. The same point has been made by Tung and Rosenthal (1985). This question was further investigated by Wiin-Nielsen (1984) with the result that energy levels comparing favorably with observations may be found, but the parameter space in which such solutions exist is quite small. One may therefore conclude that the zonal-wave interaction may not be the major mechanism at work in forming the blocking configuration.

Another possibility within low-order, nonlinear systems is that a wave-wave interaction may produce the blocking situation. This possibility was investigated by Wiin Christensen (1985) with positive results although the energy levels were too high when considering large meridional scales. A preliminary investigation of this idea was presented by Wiin-Nielsen (1986), but the system employed for the investigation was reduced to only

3 nonlinear equations by neglecting the beta-term in the vorticity equation and working solely with the cosine components of the waves, meaning that only the imaginary part of the amplitude is different from zero. Although the results were very promising, it is a severely restricted system, and one of the purposes of this paper is to present a somewhat more general analysis of wave-wave interactions. Another result of the investigation of the restricted system was that the topographical effect is of minor importance compared to the Newtonian forcing. We shall therefore not include the mountain effect in the present study. Benzi et al. (1986) have also investigated wave-wave interactions, but they consider only self-interactions to obtain the so-called bent resonances.

Legras and Ghil (1985), using models with 20 to 30 degrees of freedom, investigated the connections between persistent anomalies, of which blocking is an example, and atmospheric predictability. The same connection, but in an operational setting, was studied by Tracton (1990) because of errors in some global predictions models with respect to the formation and duration of blocks. Buzzi et al. (1986) reinvestigated the Charney-DeVore model to provide observational evidence for the multiple steady state theory and improved the model to contain the bent resonance by including selfinteraction by waves.

The synoptic development leading to blocking was already described by Berggren et al. (1949), and from that description one may easily see that at least some blocking situations appear to develop as a series of developing and interacting waves move across the Atlantic gradually producing the blocking situation in the eastern part of the Atlantic or over Scandinavia. However, the role of the zonal flow in these developments is unknown. Similar data studies were included in the paper by Tracton (1990) referenced above.

Thompson (1957) has contributed to the understanding of the long term velocity variations in barotropic flow by providing a theory for the time variations of the zonal flow as influenced by the statistics of the eddy behavior. The theory is entirely internal in the sense that heating, topographical effects and friction play no rôle in it. Additional comments on the theory may be found in the paper by Wiin-Nielsen (1986) containing examples of integrations of Thompson's equation in time for various cases. It is evident that jets with sufficiently strong horizontal shear will in time be divided in jets containing two branches. The theory provides therefore a mechanism that is capable of producing the split in the jet stream that is also an important feature of the blocking pattern. On the other hand, the theory does not give a complete description of the formation of the blocking high simply because it deals entirely with the zonally averaged flow.

It is well known that an analytical-numerical study of nonlinear systems becomes very cumbersome as soon as the number of components increases. The major problem is the determination of the multiple steady states. In this study, we shall therefore restrict ourselves to the interaction between three waves in a equivalent barotropic system with Newtonian forcing. In the real domain we will thus have a system of six nonlinear equations. The determination of the steady states is cumbersome, but it can be accomplished by characterizing the waves by the amplitude and the phase replacing the amplitudes of the sine and cosine components of the wave. Furthermore, the analysis is simplified if we assume that the forcing is restricted to only two of the three components.

Using such a limited system we cannot hope to describe the details of blocking phenomena. We may hope to show that the wave-wave interaction is a definite mechanism at work in the formation of some of the quasi-stationary flow patterns that we call blocking situations. As we shall see in the description of the investigation, it is at the same time difficult to obtain the energy levels and the horizontal scales characteristic of blocking but in spite of the difficulty the theory does describe some major aspects of the phenomenon.

2. The model

The basic equation is the equivalent barotropic vorticity equation. Using the radius of the Earth, a, as the length scale and Ω^{-1} as the time scale, with Ω denoting the angular velocity of the rotation of the Earth, we may write the basic equation in the form:

$$\partial\nabla^2\psi/\partial t = J(\nabla^2\psi, \psi) - 2(\partial\psi/\partial\lambda) - \Gamma(\psi - \psi^*), \tag{2.1}$$

where ψ is the streamfunction, ψ^* the forcing streamfunction and Γ the intensity of the Newtonian forcing. (2.1) is transformed to the wave number space following Platzman (1962) and using his notation results in the spectral equation:

$$\frac{d\psi_\gamma}{dt} = \frac{1}{2} i \sum_\beta \sum_\alpha \frac{C_\beta - C_\alpha}{C_\gamma} K(\gamma, \beta, \alpha)\, \psi_\beta \psi_\alpha + i \frac{2l_\gamma}{C_\gamma} \psi_\gamma - \Gamma(\psi_\gamma - \psi_\gamma^*), \tag{2.2}$$

where $K(\gamma, \beta, \alpha)$ is the interaction coefficient, l the nondimensional wavenumber and $c = n(n+1)$.

The components in the series development of the streamfunction are of the form:

$$\psi = \hat{\psi} P_n^l(\mu)\, e^{il\lambda}, \tag{2.3}$$

where the amplitude is a complex number that we shall write in the form:

$$\hat{\psi} = \tfrac{1}{2}(x - iy), \tag{2.4}$$

from which it follows that the longitude dependent part of the wave can be written as:

$$x \cos(l\lambda) + y \sin(l\lambda) \tag{2.5}$$

As Platzman (1962), we shall make use of the complex wave number recalling that both wave number and its conjugate should be included in the model. We select three waves in such a way that the selection rules are satisfied. After some calculations we obtain the following six equations in the real domain:

$$\frac{dx_1}{dt} = -\frac{1}{2} g_1 (x_2 y_3 - x_3 y_2) - \frac{2l_1}{C_1} y_1 - \Gamma(x_1 - x_1^*), \tag{2.6}$$

$$\frac{dy_1}{dt} = \frac{1}{2} g_1 (x_2 x_3 + y_2 y_3) + \frac{2l_1}{C_1} x_1 - \Gamma(y_1 - y_1^*), \tag{2.7}$$

$$\frac{dx_2}{dt} = -\frac{1}{2} g_2 (x_1 y_3 - x_3 y_1) - \frac{2l_2}{C_2} y_2 - \Gamma(x_2 - x_2^*), \tag{2.8}$$

$$\frac{dy_2}{dt} = \frac{1}{2} g_2 (x_1 x_3 + y_1 y_3) + \frac{2l_2}{C_2} x_2 - \Gamma(y_2 - y_2^*), \tag{2.9}$$

$$\frac{dx_3}{dt} = \frac{1}{2} g_3 (x_1 y_2 + x_2 y_1) - \frac{2l_3}{C_3} y_3 - \Gamma(x_3 - x_3^*), \tag{2.10}$$

$$\frac{dy_3}{dt} = -\frac{1}{2} g_3 (x_1 x_2 - y_1 y_2) + \frac{2l_3}{C_3} x_3 - \Gamma(y_3 - y_3^*). \tag{2.11}$$

The following symbols have been introduced:

$$g_1 = \frac{C_2 - C_3}{C_1} K, \qquad g_2 = \frac{C_3 - C_1}{C_2} K, \qquad g_3 = \frac{C_1 - C_2}{C_3} K. \tag{2.12}$$

The first problem is to search for the steady state solutions of the coupled nonlinear equations. It turns out that the most convenient procedure is to replace the two amplitude components by a single amplitude and a phase angle by writing

$$x = R \cos\theta, \quad y = R \sin\theta, \qquad x^* = R^* \cos\theta^*, \quad y^* = R^* \sin\theta^*, \tag{2.13}$$

with the proper subscripts in each case. In addition we introduce the notations:

$$F = \frac{2l}{C}. \tag{2.14}$$

It is then a straightforward matter to derive the equations for the rate of change of the amplitudes and the phase angles. In this connection it is an advantage to introduce the notation:

$$\phi = \theta_1 + \theta_2 - \theta_3. \tag{2.15}$$

The first system of 6 equations is then replaced by another system with the same number of equations. They are:

$$\frac{dR_1}{dt} = \frac{1}{2} g_1 R_2 R_3 \sin\phi - \Gamma R_1 + \Gamma R_1^* \cos(\theta_1^* - \theta_1), \tag{2.16}$$

$$R_1 \frac{d\theta_1}{dt} = \frac{1}{2} g_1 R_2 R_3 \cos\phi + F_1 R_1 + \Gamma R_1^* \sin(\theta_1^* - \theta_1), \tag{2.17}$$

$$\frac{dR_2}{dt}=\frac{1}{2}g_2R_1R_3\sin\phi$$
$$-\Gamma R_2+\Gamma R_2^*\cos(\theta_2^*-\theta_2), \tag{2.18}$$
$$R_2\frac{d\theta_2}{dt}=\frac{1}{2}g_2R_1R_3\cos\phi$$
$$+F_2R_2+\Gamma R_2^*\sin(\theta_2^*-\theta_2), \tag{2.19}$$
$$\frac{dR_3}{dt}=\frac{1}{2}g_3R_1R_3\cos\phi$$
$$-\Gamma R_3+\Gamma R_3^*\cos(\theta_3^*-\theta_3), \tag{2.20}$$
$$R_3\frac{d\theta_3}{dt}=-\frac{1}{2}g_3R_1R_2\cos\phi$$
$$+F_3R_3+\Gamma R_3^*\sin(\theta_3^*-\theta_3). \tag{2.21}$$

The steady state equations have been solved in a special case only. It has been assumed that the forcing is nonzero on only two of the waves, while the third has been assumed to vanish. In the case treated below it has been assumed that the middle component forcing is zero. In that case it follows from (2.18) and (2.19) that

$$\cos\phi=-\frac{2F_2R_2}{g_2R_1R_3},\qquad \sin\phi=\frac{2\Gamma R_3}{g_2R_1R_3}. \tag{2.22}$$

It is seen from (2.22) that

$$\sin^2\phi+\cos^2\phi=\frac{4(\Gamma^2+F_2^2)}{g_2^2}\frac{R_2^2}{R_1^2R_3^2}=1,\qquad \tan\phi=\frac{\Gamma}{-F_2}. \tag{2.23}$$

The strategy is then to introduce the expressions in (2.23) in (2.16), (2.17), (2.20) and (2.21). Denoting

$$\gamma_1=\theta_1^*-\theta_1,\qquad \gamma_3=\theta_3^*-\theta_3, \tag{2.24}$$

and

$$Q_1=\frac{-g_2g_2}{4(\Gamma^2+F_2^2)},\qquad Q_3=\frac{-g_2g_3}{4(\Gamma^2+F_2^2)}. \tag{2.25}$$

We may first write the 4 equations in the form:

$$\begin{aligned}R_1^*\cos\gamma_1&=R_1(1+Q_1R_3^2),\\ R_1^*\sin\gamma_1&=-R_1(F_1/\Gamma+Q_1F_2R_3^2/\Gamma),\\ R_3^*\cos\gamma_3&=R_3(1+Q_3R_1^2),\\ R_3^*\sin\gamma_3&=-R_3(F_3/\Gamma-Q_3F_2R_1^2/\Gamma).\end{aligned} \tag{2.26}$$

Squaring and adding the first two and thereafter the last two equations in (2.26) and denoting

$$N^2=(1+Q_3R_1^2)^2+\frac{F_3^2}{\Gamma^2}\left(1-Q_3\frac{F_2}{F_3}R_1^2\right)^2, \tag{2.27}$$

we may finally write an equation having only one unknown. It is:

$$Z\left[\left(1+Q_1\frac{R_3^{*2}}{N^2}\right)^2+\frac{F_1^2}{\Gamma^2}\left(1+Q_1\frac{F_2}{F_1}\frac{R_3^{*2}}{N^2}\right)^2\right]=R_1^{*2},\qquad Z=R_1^2. \tag{2.28}$$

The procedure of solution is then first to solve (2.28) for the variable Z using a standard root finding routine. For each of the roots in (2.28) we proceed to find the remaining variables from the following expressions:

$$R_3=R_3^*/N,\qquad \tan\gamma_1=\frac{-F_1}{\Gamma}\frac{1+Q_1F_2R_3^2/F_1}{1+Q_1R_3^2},\qquad \tan\gamma_3=\frac{-F_3}{\Gamma}\frac{1-Q_3F_2R_1^2/F_3}{1+Q_3R_1^2}, \tag{2.29}$$

$$\tan\phi=\frac{\Gamma}{-F_2},\qquad \theta_1=\theta_1^*-\gamma_1,\qquad \theta_3=\theta_3^*-\gamma_3,\qquad \theta_2=\phi+\theta_3-\theta_1 \tag{2.30}$$

Tellus A/48/2-5

3. Results

The formulation given in the previous section can be applied to any combination of three waves. Using the selection rules it is necessary to obtain an interaction coefficient that is different from zero, since otherwise the system is linear and thus uninteresting for the purposes of the present investigation. The system has been studied (Wiin Christensen, 1985) with respect to the horizontal scales of the three components. It became evident that if the three components are of large meridional scale the resulting solutions will have kinetic energy amounts far exceeding those observed in real blocking situations (Schilling, 1986). This feature of the solutions is understandable from the fact that a blocking high has a limited size in the meridional direction. Due to the divided jetstream with branches going north and south of the blocking high one finds low geopotential regions to the north and the south of the middle latitude high. Combined with the fact that the tropical region is undisturbed it is necessary to select associated Legendre functions with several zeroes between pole and equator.

At the same time as shown from observations by Austin (1980) it appears likely that blocking situations are created by an interaction between the planetary longitudinal wave numbers 1, 2 and 3 representing a triplet satisfying the longitudinal part of the selection rules. The second index in the associated Legendre function must then be selected in an appropriate way. We shall follow this strategy. Based on these considerations and the earlier experiments we have selected a triplet where the indices on the associated Legendre functions are (3, 13), (1, 10) and (2, 12) listed in this order because we choose to have the forcing on longitudinal wave numbers 3 and 2 with no forcing on wave number 1. These selections are very realistic when compared to the real atmosphere since the basic selection of (1, 10) gives 5 zeroes between pole and equator. This can be interpreted as representing a classical blocking situation. Experiments show that the kinetic energy levels are sensitive to the choice of the coefficient Γ. The results obtained here used a value for the non-dimensional coefficent $\Gamma = 0.005$.

The equations needed to calculate solutions to the problem are (2.27)–(2.30). To solve the steady state problem we must find solutions to (2.28) using the expression in (2.27). The first difficulty is to obtain an understanding of the conditions under which (2.28) has multiple solutions. For this to be possible it is seen that the function on the left hand side of (2.28) should have at least one maximum and one minimum. If, we, for a given value of

$$z_{3s} = R_3^{*2}, \tag{3.1}$$

can find the maxima and minima of the left hand side of (2.28) we then know the interval of

$$z_{1s} = R_1^{*2} \tag{3.2}$$

for which multiple solutions are possible.

It is furthermore seen that the function in question is an entirely positive function since z by definition is positive and the quantity in square brackets is a sum of squared quantities. The function is furthermore zero for $z = 0$, and it will therefore have a positive derivative for $z = 0$. The determination of the positions of the maxima and minima are obtained by an elementary calculation of the derivative followed by a numerical determination of the roots of the equation obtained by setting the derivative equal to zero. Standard numerical root finding routines are used for this purpose.

It would be possible to determine all positive roots in the equation, but we shall limit ourselves to the roots corresponding to relatively small values of the kinetic energy in the three components. The kinetic energy of a given component, expressed in energy per unit area, is obtained by integrating the kinetic energy per unit mass over the whole area of the sphere and dividing the result by the total area: $4\pi a^2$. After integration we obtain:

$$K = \frac{1}{8}\frac{p_0}{g} a^2 \Omega^2 cz,$$

$$c = n(n+1), \tag{3.3}$$

$$z = R^2.$$

Evaluating the formula in (3.3) for the component with the largest value of c we find that it will be sufficient to look for roots with a value less than 4, when we scale the value of z by the factor 10^{-5}. Looking first at the positions and the values of the

extrema of the function we find that multiple solutions are possible only when

$$z_{3s} \geqslant 18. \tag{3.4}$$

Fig. 1 shows the values of the maxima and the minima as a function of z_{3s}. The values of z_{1s} must for each value of z_{3s} be selected between the minimum and the maximum values to obtain multiple solutions. It will be seen that close to the limit given by (3.4) there are narrow limits for the selection of z_{1s}, but as z_{3s} increases a much wider choice is available for the selection of the intensity of the forcing given by z_{1s}. It would thus appear that blocking situations may be created by a large number of combinations of forcing functions. However, this statement is acceptable only if the necessary condition that the energy amounts of a given solution are of the same order of magnitude as the amounts shown by data studies. Due to the simplicity of the model, one cannot expect a close agreement with the observed situations.

Fig. 2 gives the energy levels for the blocked state as the dashed curve. They are high, but of the correct order of magnitude. The non-blocked state is given in the same diagram as the full curve. The energies displayed by the curves is the sum of the energies on all three components contained in the steady state. Fig. 3 shows a different case where the value of z_{1s} has been reduced from $z_{1s} = 50.0$ (scaled value) to $z_{1s} = 30.0$. It is seen that the energy levels for the blocked state are considerably lower in the case of lower forcing.

The stability of the various steady states is important. As seen from Fig. 1 it is necessary to have z_{3s} at a sufficiently high level before multiple steady states will appear. When they do we find in general three steady states for values of $z_1 < 4$. To investigate the stability one may return to the original 6 equations, i.e., (2.6) to (2.11). Following standard procedures for linearization one may derive the perturbation equations for small deviations from a given steady state. Writing all the perturbation variables in the form:

$$(x, y) = (x_0, y_0) \exp(\nu t), \tag{3.5}$$

one may reduce the stability problem to a standard eigenvalue problem that has been solved numerically by standard procedures. The main result of the stability investigations is that the steady states corresponding to the smallest and the largest values of z_1 are stable, while the middle value is unstable. We stress that to perform the stability investigation it is necessary to calculate the values of z_2 and z_3 as well as the phase angles correspond-

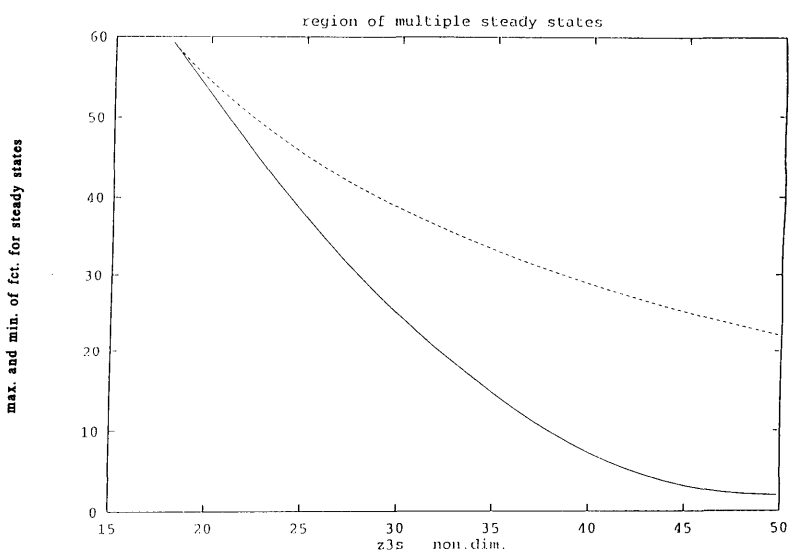

Fig. 1. The region of multiple steady states is between the two curves. The ordinate is also the forcing on wave component 1.

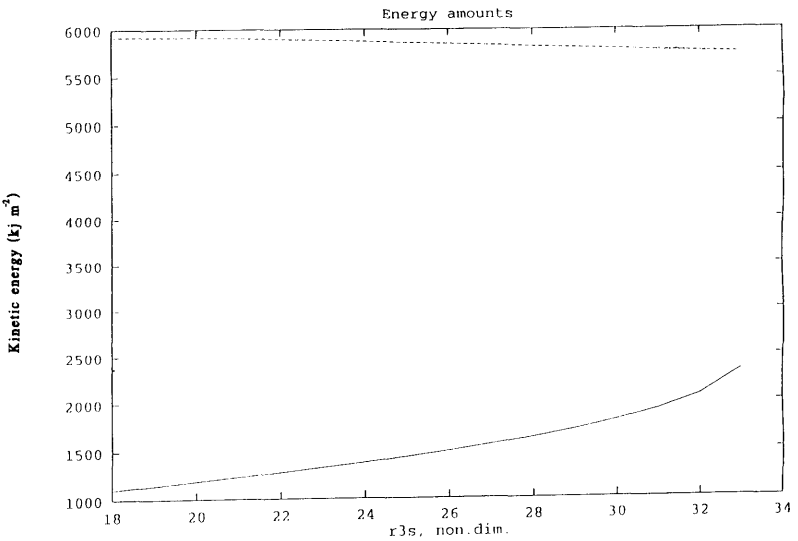

Fig. 2. Energy levels. Dashed curve is for the blocked states, full curve for the stable unblocked states.

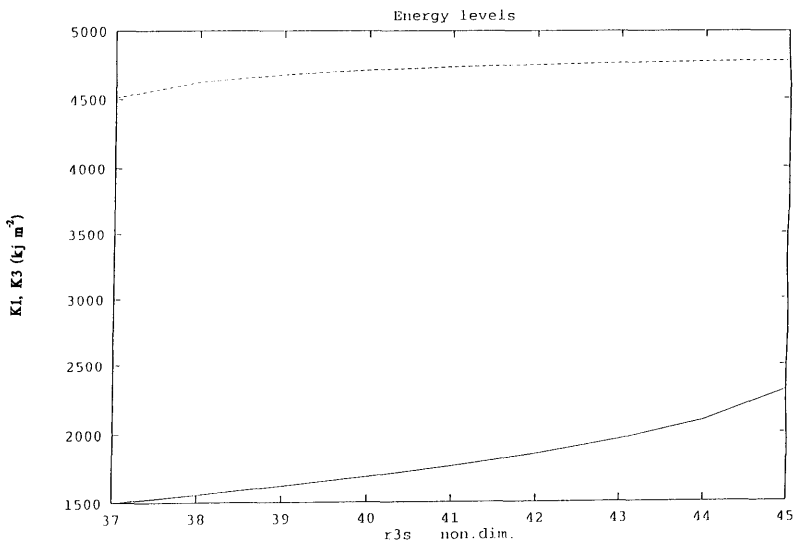

Fig. 3. As Fig. 2 except that the forcing on wave component 1 has been reduced from 50 to 30 units (scaled values).

ing to all three values of z. The formulas are given in Section 2. It has not been found necessary to reproduce all the calculations here, but it may be of interest to give an example.

Fig. 4, calculated with $z_{1s} = 50.0$ and $z_{3s} = 21.025$, shows the position of the three roots as the intersections with the zero line. The kinetic energies corresponding to the first stable steady state are $K1 = 931$ kJ m^{-2}, $K2 = 210$ kJ m^{-2} and $K3 = 882$ kJ m^{-2}, while those attached to the second stable steady state are $K1 = 1628$ kJ m^{-2}, $K2 = 679$ kJ m^{-2} and $K3 = 1634$ kJ m^{-2}. The blocking case has thus a total energy amount corresponding to almost twice the amount in the non-blocked case. In Fig. 5 we show the blocking case at 40 N together with the forcing (dashed curve). Wave numbers 2 and 3 cooperate to form the largest ridge in the middle of the figure. Only small amplitude ridges are formed to the west and the east of the large amplitude ridge. Fig. 6 is the non-blocked case with smaller amplitudes located at almost the same longitudes. The present case corresponds to a single block of the Pacific type according to Austin (1980), since the forcing amplitudes are large on wavenumbers two and three. It happens when the largest forcing is 40 to 50° to the west of the position of the block in this case. Figs. 5, 6 have $r_{1s} = 50$, $\theta_{1s} = -90°$ and $r_{3s} = 21.025$, $\theta_{3s} = -45°$, where the r values are given in scaled form. Figs. 7, 8 show in a similar arrangement a case, where $r_{1s} = r_{3s} = 30$, while $\theta_{1s} = -90$ and $\theta_{3s} = -55°$. The latter case displayed in Figs. 7, 8 show a larger difference between the blocked and the non-blocked case.

Due to the stability present in the two solutions with the smallest and the largest energy levels the system will display a form of hysteresis. To demonstrate this we start an integration (Fig. 9) with a forcing so small that only one stable low energy state exists. We let the forcing in the experiment increase slowly with time. It will after a while be so large that three steady states will be possible, but the low energy state is stable, and the system will therefore stay in that state. However, when the forcing becomes so large that the system moves out of the region with multiple steady states, there will be only one steady state, i.e. the high energy stable steady state. At this point we discontinue the increase in the forcing. The system will therefore fall into this steady state after some additional time. The calculation is then continued with decreasing values of the forcing. The system will also stay in the high energy state through the region of multiple steady states. When the forcing

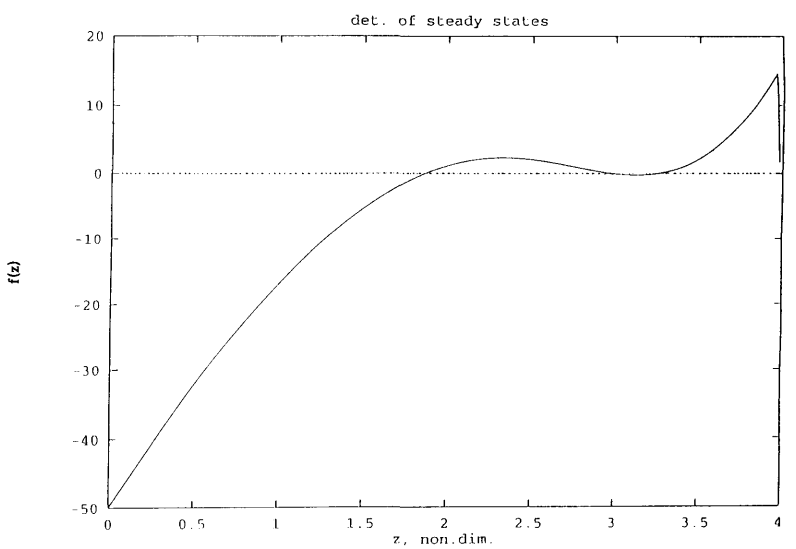

Fig. 4. An example of the determination of the three steady states. The curve is calculated for $r_{1s} = 50$ and $r_{3s} = 21.025$ (scaled values)

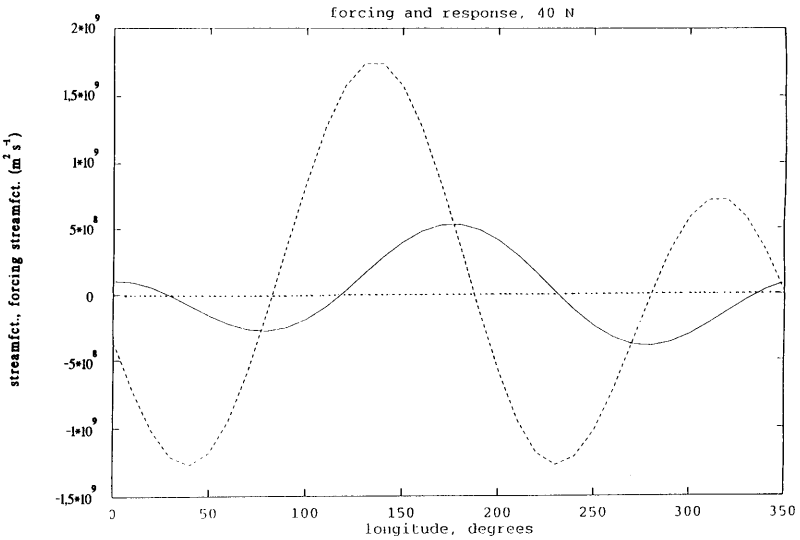

Fig. 5. The streamfunction as a function of latitude at 40 N together with the forcing streamfunction (dashed curve) for the blocked case ($r_{1s} = 50$, $r_{3s} = 21.025$).

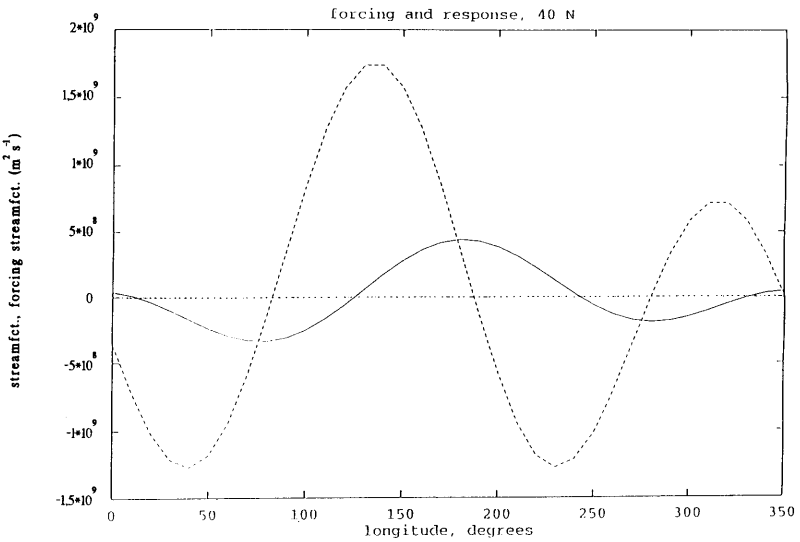

Fig. 6. As Fig. 5, but for the stable, unblocked case.

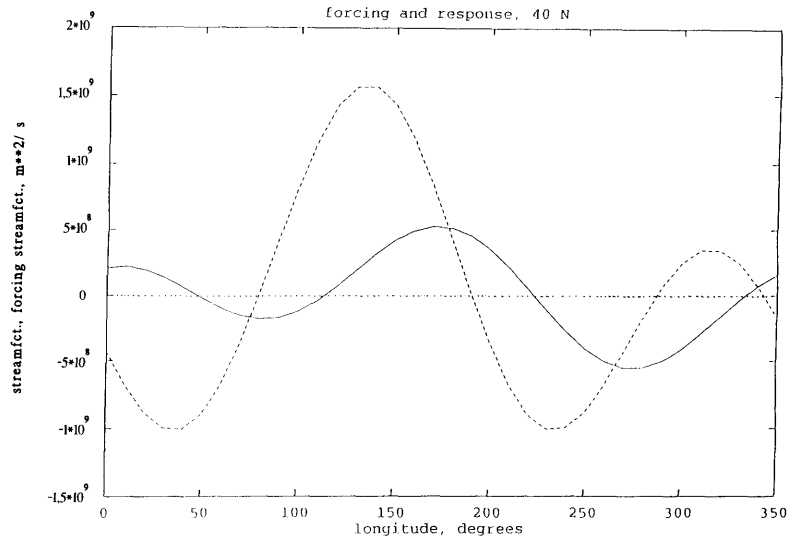

Fig. 7. As Fig. 5, but with $r_{1s} = r_{3s} = 30$.

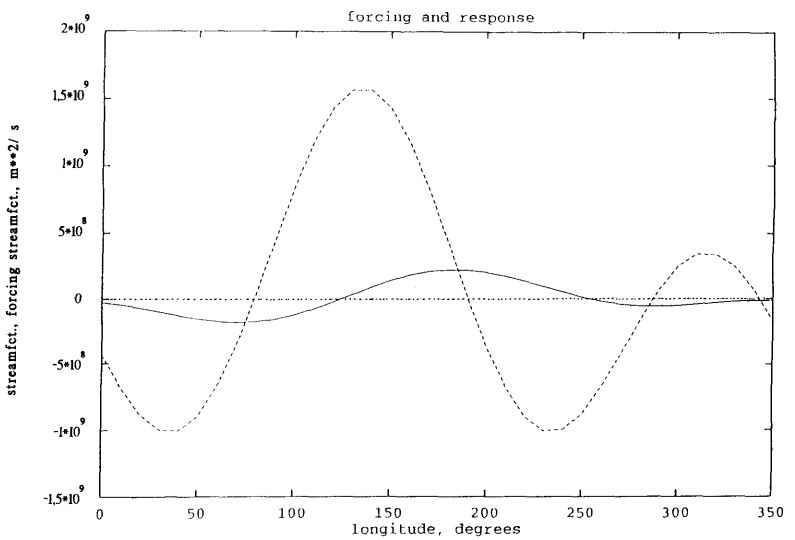

Fig. 8. As Fig. 7, but for the unblocked case.

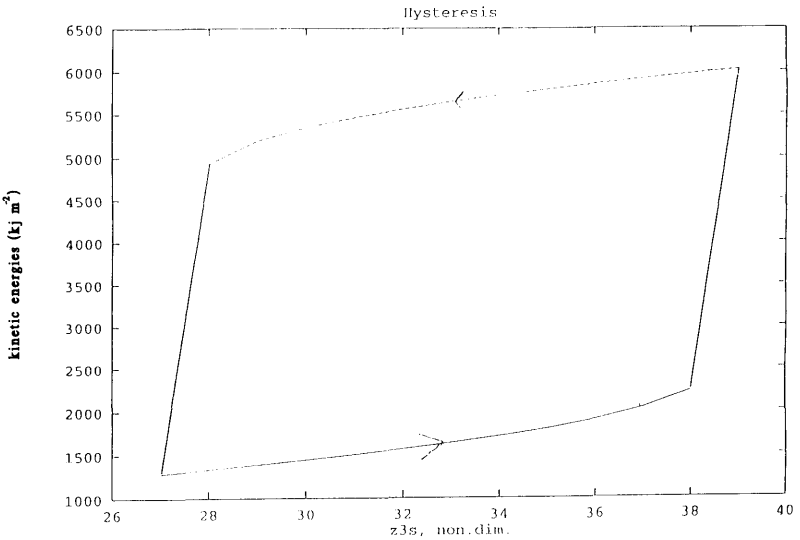

Fig. 9. The hystereris experiment with forcing on the abscissa and kinetic energy on the ordinate.

becomes so small that the system leaves the region of multiple steady states only the low energy stable steady state will exist. The system will therefore finish in this state whereby the loop is closed.

In the hysteresis experiment we come from a low to a high energy state and vice versa by increasing and thereafter decreasing the forcing. This mechanism is different from the proposals made by Speranza (1986) who considers the problem of how the system can come from the unblocked to the blocked steady state under *constant* forcing. In such a case it is proposed that stochastic disturbances are necessary to move the system from one state to another. The exit times computed from the stochasic considerations are quite realistic, and it may very well be that both mechanisms are at work.

4. Other solutions

The solutions considered in the previous sections have emphasized the multiple steady states with similarities to blocking. It has been noted that such solutions require a special specification of the forcing parameters. Such solutions are the exceptions rather than the rule for the system. In most cases one will obtain a single stable, steady state. Such solutions are easily obtained by either a long term numerical integration of the system or by using a form of Newtons method applicable to systems of equations. The latter method is to be prefered since it in principle can provide multiple solutions although it is well known that these numerical methods require a good first guess to obtain a given steady state.

In searching for multiple steady states it was discovered that for certain values of the forcing parameters the system goes into a state which can best be described as a limit cycle. We shall illustrate this behavior by an example. Let the forcing parameters be $x_1^* = -1.0$, $x_2^* = 19.0$ and $x_{3*} = 29.0$, while all forcing quantities on the y-components are zero. A numerical integration of this system from an initial state where all components are zero will finish in a limit cycle. Fig. 10 shows the components x_1 and y_1 as a function of time. The figure indicates clearly that the system for these two components will end in a closed curve. The same is the case for the components x_2, y_2 and x_3, y_3 as shown in Figs. 11, 12. An inspection of the time dependence shows that the period in the cycle is about 36 days. Plaut and Vautard (1994) have found a similar oscillation with a

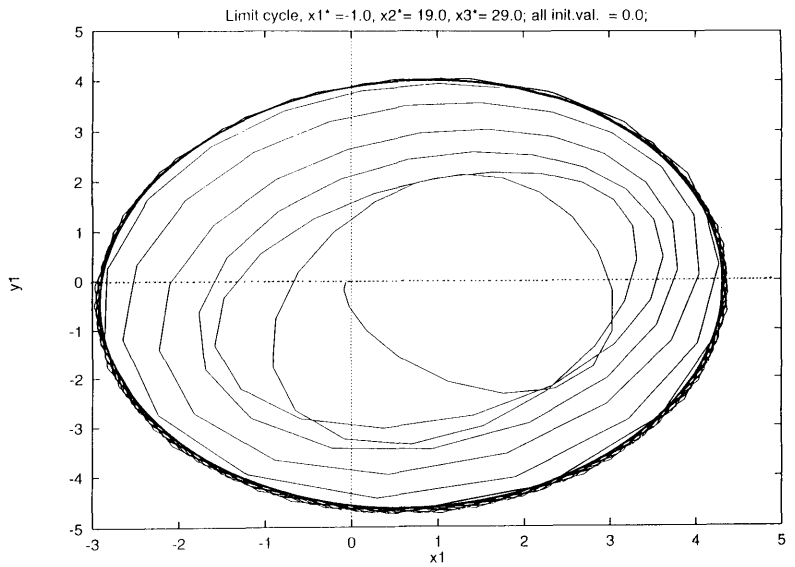

Fig. 10. Limit cycle for the following forcing. $x_1^* = -1.0$, $x_2^* = 19.0$, $x_{3^*} = 29.0$, $y_1^* = y_2^* = y_3^* = 0$. Initial conditions. all variables equal to zero. Variables along axes are x_1 and y_1.

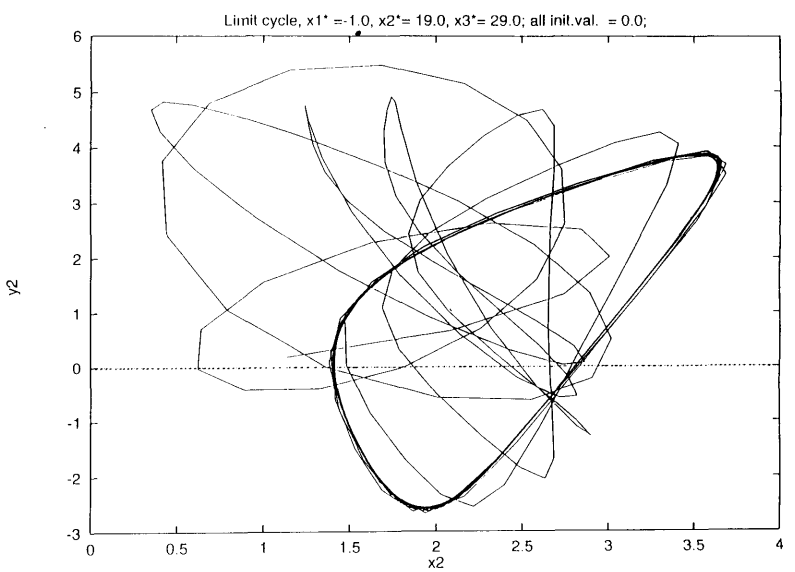

Fig. 11. As Fig. 10, but for x_2 and y_2.

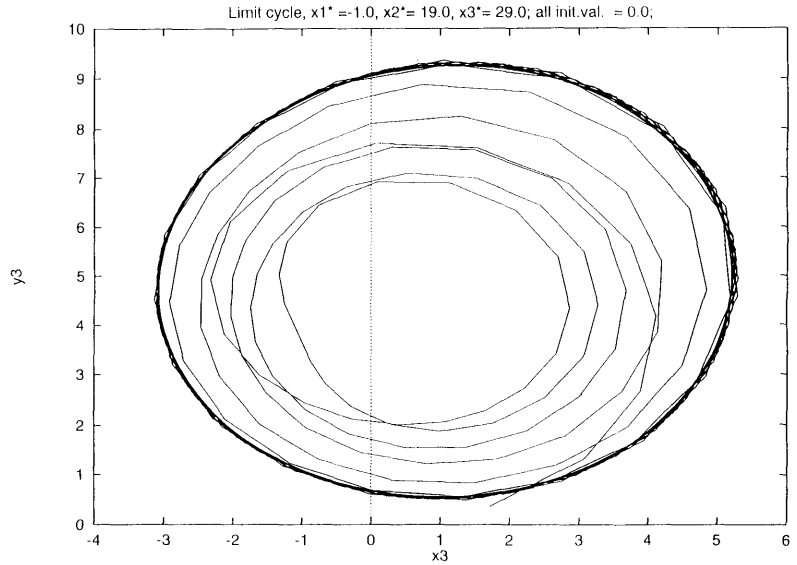

Fig. 12. As Fig. 10, but for x_3 and y_3.

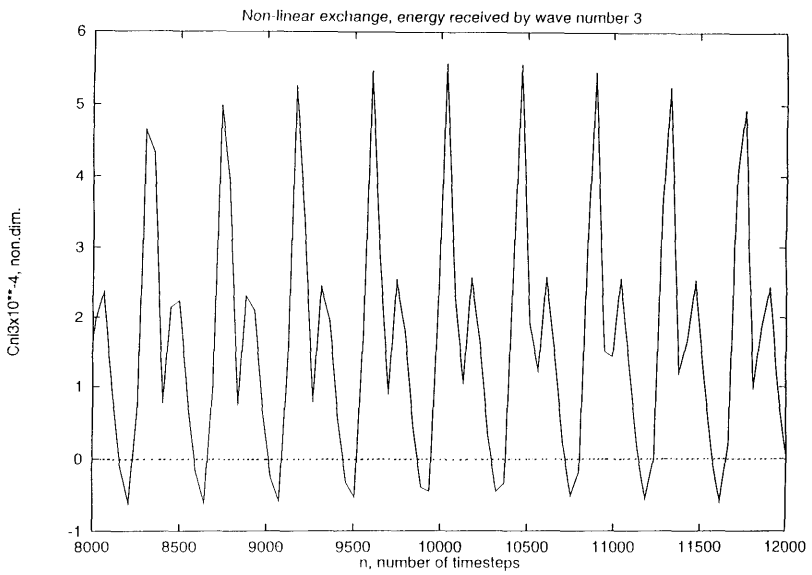

Fig. 13. Nonlinear exchange energy received by wave number 1.

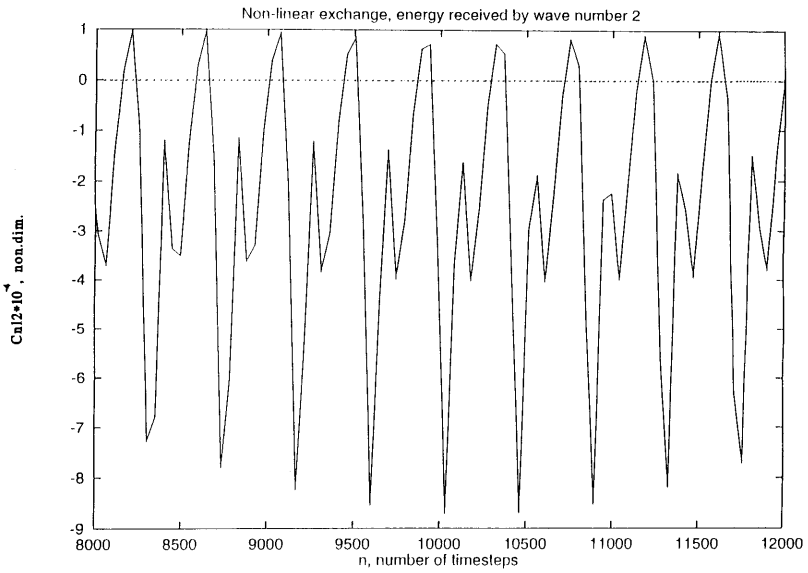

Fig. 14. Nonlinear exchange energy received by wave number 2.

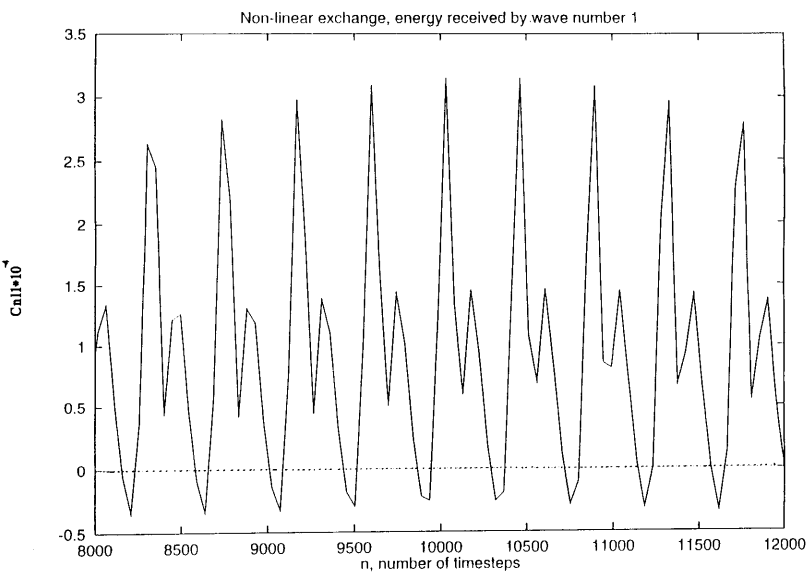

Fig. 15. Nonlinear exchange energy received by wave number 3.

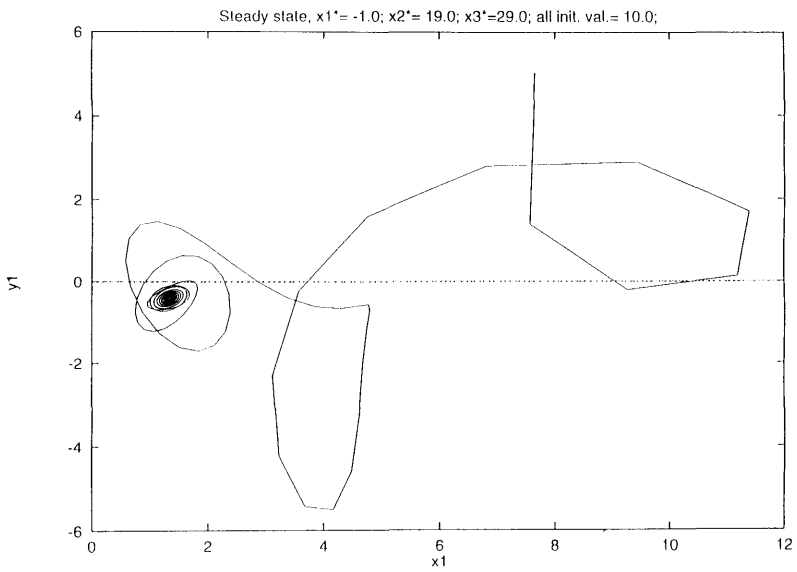

Fig. 16. Same forcing as in Fig. 10, but initial values are 10.0 for all variables. A steady state is obtained.

period of 30–35 days across the Atlantic. The period cannot be a linear phenomenon because it is the same for the three components. It should therefore be connected with the nonlinear exchange among them. This conclusion is verified by Figs. 13, 14 and 15 where the curves show the amount of energy received by a given wave number by nonlinear exchange with the other two wave numbers. We notice that energy is received on wavenumbers 1 and 3, while a loss of energy by nonlinear interaction takes place from wavenumber 2. The period of the shorter oscillation is the same (36 days) as we found for the limit cycle. These figures indicate also that a longer period is present in the energy exchange. It is most likely due to the numerical integration scheme where rather long timesteps of 3 h have been used. A test calculation with smaller timesteps indicates that the longer period disappears.

There are, however, other types of solutions for certain forcing values. Let us for example consider the solutions for the following forcing values: $x_1^* = -1.0$, $x_2^* = 19.0$ and $x_3^* = 29.0$, while all the y-values are zero. Starting from initial values all equal to 10.0 we find that the solution approaches a steady state as illustrated by Fig. 16. If we, on the other hand, start from an initial state, where all the variables are set to zero we know that a limit cycle exists (Fig. 10). We have thus very different behaviors of the system depending on the starting position. It would be of interest to determine the set of starting values leading to limit cycles and those resulting in a steady state. However, such a mapping of the six-dimensional space is far from easy and goes beyond the purpose of this paper.

5. Concluding remarks

Several proposals have been made for the creation of blocking situations since the first studies in 1979. In addition to the various proposals involving multiple steady states there are suggestions pointing to solitary waves (modon) models (Hains, 1987) and dipole models (McWilliams, 1980) as possible mechanisms. All of the proposals are based on very simple low order models, and none of them are able to match the specific conditions of natural blocks. Källén (1981, 1982) has shown that results in a low order equivalent barotropic model with respect to blocking can be reproduced in a numerical integration of a higher order model af the same kind. For his experiment to be realistic it was, however, necessary to increase the (thermal) forcing, because otherwise the cascade of energy to the smaller scales would

prevent creation of the block. This experiment may indicate why there is such a discrepancy between the energy levels of the blocked state in low order models as compared to natural blocks. In low-order models the energy is trapped in the modes permitted in the model, while a high-order model will cascade energy to the larger wave numbers. In an operational global model (Simmons, 1986) it was found that the treatment of blocking appears to pose no outstanding problem. Cases of high predictability involving blocks have been noted as for example described by Bengtsson (1981). While the latter study points out that high resolution models perform better in predicting blocks than models with lower resolutions, it is also mentioned that models with moderate resolution still clearly indicate the formation of the blocks although lacking in detail.

The present proposal (that wave-wave nonlinear interaction may be an essential part of the creation of some blocking patterns) is partly based on the larger agreement with the observed energy amounts and partly on the more realistic wave forcing both with respect to magnitude and position as indicated by the relation between the forcing and the resulting block.

6. Appendix

A particularly simple case of the low order system under consideration in this paper is obtained if one neglects the Coriolis force and includes only the sine components of the waves in the description. One observes that in this case the system reduces to the much simpler three component system:

$$\frac{dy_1}{dt} = \frac{1}{2} g_1 y_2 y_3 + \Gamma(y_1^* - y_1),$$

$$\frac{dy_2}{dt} = \frac{1}{2} g_2 y_1 y_3 + \Gamma(y_2^* - y_2), \tag{17}$$

$$\frac{dy_3}{dt} = \frac{1}{2} g_3 y_1 y_2 + \Gamma(y_3^* - y_3).$$

Although of lesser relevance to the real atmosphere than the six component system because of the neglect of the Coriolis terms, the above system displays many of the features of the more general system. In the present case it is possible to determine the stationary states with an arbitrary forcing. By solving the last two equations in (17) for y_2

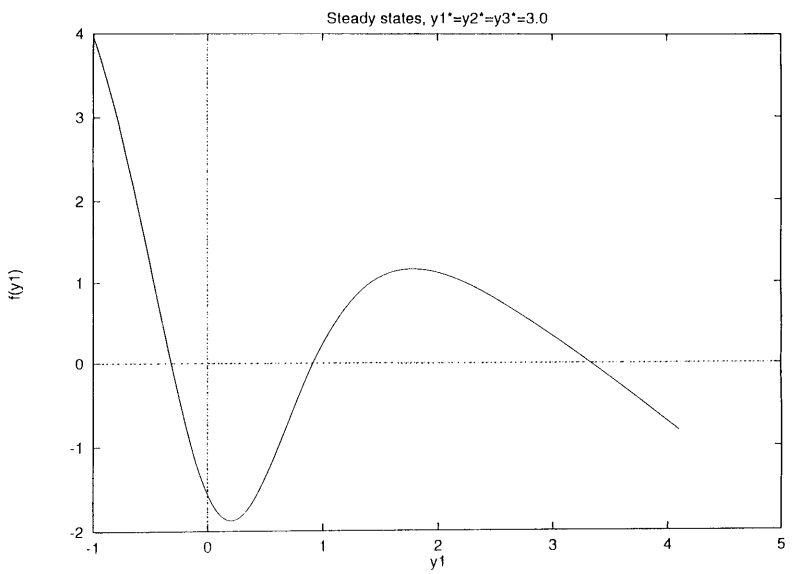

Fig. 17. Steady states in the low order model with three variables for $y_1^* = y_2^* = y_3^* = 3.0$.

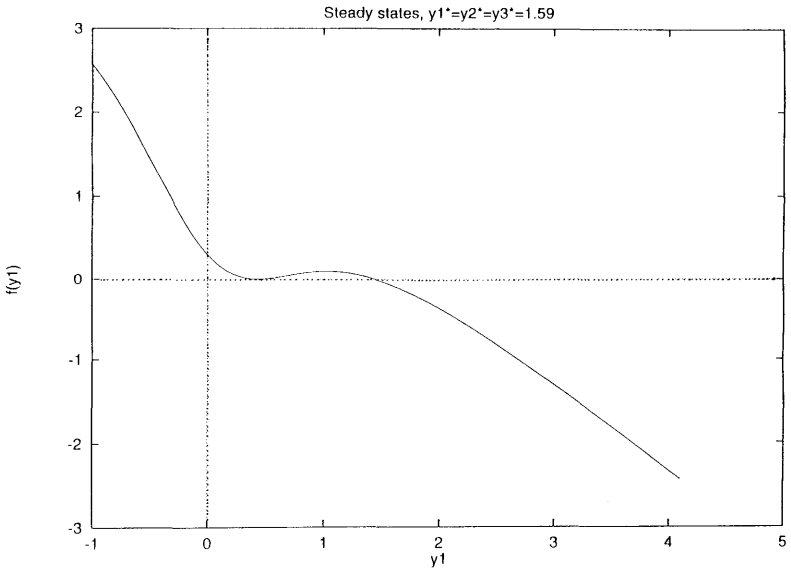

Fig. 18. As Fig. 17, but all three forcing variables are 1.59.

and y_3 for the steady state equations and inserting the resulting expressions in the first equation of (17) with $\mathrm{d}/\mathrm{d}t = 0$ we obtain the following equation for y_1:

$$a_1(y_2^* + a_2 y_3^* y_1)(y_3^* + a_3 y_2^* y_1) + (y_1^* - y_1(1 - a_2 a_3 y_1^2)^2 = 0, \qquad (18)$$

$$a_i = \frac{g_i}{2\Gamma}; \qquad i = 1, 2, 3.$$

It is seen that (18) is a 5th degree equation that may be solved by numerical methods. In each case we have found that the roots are either two conjugate complex roots and three real roots or two pairs of conjugate complex roots and one real root. The system (17) may thus have one or three steady states. Plotting the left hand side of (18) against y_1 one may locate the roots by inspection. In the case of three real roots for y_1 it turns out that the steady state corresponding to the middle root is unstable while the other two steady states are stable. The case of a single steady state is normally obtained for sufficiently low values of the three forcing parameters y_i^*. These situations are described in the Figs. 17 and 18. In Fig. 17 we have three steady states, while Fig. 18 shows a case where the forcing is such that the two steady states to the left are about to disappear.

The special case considered in this appendix indicates that it behaves in many respects in the same way as the more complicated system containing 6 equations. On the other hand, it is no more than an example, and the results are not directly applicable to the atmosphere.

REFERENCES

Austin, J. F. 1980. The blocking of middle latitude westerly winds by planetary waves. *Q. J. Roy. Met. Soc.*, **106**, 327–350.

Bengtsson, L. 1981. Numerical prediction of atmospheric blocking. A case study. *Tellus* **33**, 19–42.

Benzi, R., Malguzzi, P., Speranza, A. and Sutera, A. 1986. The statistical properties of general atmospheric circulation. Observational evidence and a minimal theory of bimodality. *Q. Jour. Roy. Met. Soc.* **112**, 661–674.

Benzi, R., Saltzman, B. and Wiin-Nielsen, A. (eds.). 1986. Anomalous atmospheric flows and blocking. *Adv. in Geophys.* **29**, 459 pp.

Berggren, R., Bolin, B. and Rossby, C.-G. 1949. An aerological study of zonal motion, its perturbations and breakdown. *Tellus* **1**, 14–37.

Charney, J. G. and DeVore, J. G. 1979. Multiple flow equilibria in the atmosphere and blocking. *J. Atmos. Sci.* **36**, 1205–1216.

Elliott, R. D. and Smith, T. B. 1949. A study of the effects of large blocking highs on the general circulation in the Northern Hemisphere westerlies. *Jour. Meteor.* **6**, 67–85.

Egger, J. 1978. Dynamics of blocking highs. *J. Atmos. Sci.* **35**, 1788–1801.

Hains, K. 1987. Solitary wave models of blocking persistence. *Dyn. Low. Frec. Phenom. in the Atmosphere*, 733–741.

Källén, E. 1981. The nonlinear effects of orographic and momentum forcing in a low order, barotropic model. *J. Atmos. Sci.* **39**, 2150–2163.

Källén, E. 1982. Bifurcation properties of quasi-geostrophic, barotropic models and their relation to atmospheric blocking. *Tellus* **34**, 255–265.

Legras, B. and Ghil, M. 1985. Persistent anomalies, blockings, and variations in atmospheric predictability. *J. Atmos. Sci.* **42**, 433–471.

Lejenäs, H. 1984. Characteristics of Southern Hemisphere blocking as determined from a time series of observational data. *Q. J. Roy. Met. Soc.* **110**, 967–979.

Lejenäs, H. and Økland, H. 1983. Characteristics of Northern Hemisphere blocking as determined from a long time series of observational data. *Tellus* **35A**, 350–362.

McWilliams, J. C. 1980. An application of equivalent modons to atmospheric blocking. *Dyn. Atmos. Oceans* **5**, 43–66.

Platzman, G. W. 1960. The spectral form of the vorticity equation. *Jour. Meteor.* **17**, 635–644.

Platzman, G. W. 1962. The analytical dynamics of the spectral vorticity equation. *J. Atmos. Sci.* **19**, 313–328.

Plaut, G. and Vautard, R. 1994. Spells of low-frequency oscillations and weather regimes in the Northern Hemisphere. *J. Atmos. Sci.* **51**, 210–236.

Rex, D. 1950. Blocking action in the middle troposphere and its effect on regional climate. *Tellus* **2**, 196–211, 275–301.

Schilling, H.-D. 1986. On atmospheric blocking types and blocking numbers. *Adv. in Geophys.* **29**, 71–99.

Simmons, A. J. 1986. Numerical prediction. Some results from operational forecasting at ECMWF. *Adv. in Geophys.* **29**, 305–338.

Speranza, A. 1986. Deterministic and statistical properties of Northern Hemisphere, middle latitude circulation: minimal theoretical models. *Adv. in Geophys.* **29**, 199–225.

Thompson, P. D. 1957. A heuristic theory of large-scale turbulence and long-period velocity variations in barotropic flow. *Tellus* **9**, 69–91.

Tung, K. K. and Rosenthal, A. J. 1985. Theories of multiple equilibiria: a critical reexamination. *J. Atmos. Sci.* **42**, 2804–2819.

Tracton, M.S. 1990. Predictability and its relationship to scale interaction processes in blocking. *Mo. Wea. Rev* **118**, 1666–1695.

Vickroy, J. G. and Dutton, J. A. 1979. Bifurcation and catastrophe in a simple, forced, dissipative quasi-geostrophic flow. *J. Atmos. Sci.* **36**, 42–52.

Wiin Christensen, C. 1985. *Blocking.* M.Sc diss., Geophysical Dept., University of Copenhagen, Denmark, 106 pp.

Wiin-Nielsen, A. 1979. Steady states and stability properties of a low-order, barotropic system with forcing and dissipations. *Tellus*, **31**, 375–386.

Wiin-Nielsen, A. 1984. Low and high index steady states in a low order model with vorticity forcing. *Contrib. Phys. Free Atmos.* **57**, 291–306.

Wiin-Nielsen, A. 1986. Global scale circulations: a review. *Adv. in Geophys.* **29**, 3–27.